


Article

Diatomite and Glucose Bioresources Jointly Synthesizing Anode/Cathode Materials for Lithium-Ion Batteries

Yun Chen ^{1,2}, Bo Jiang ¹, Yue Zhao ³, Hongbin Liu ^{4,*}  and Tingli Ma ^{1,3,*}

¹ Graduate School of Life Science and Systems Engineering, Kyushu Institute of Technology, 2-4 Hibikino, Wakamatsu, Kitakyushu 808-0196, Japan

² Medical Engineering and Technology Research Center, School of Radiology, Shandong First Medical University & Shandong Academy of Medical Sciences, Taian 271000, China

³ College of Materials and Chemistry, China Jiliang University, Hangzhou 310018, China

⁴ School of Materials Science and Engineering, Harbin Institute of Technology (Shenzhen), Shenzhen 518055, China

* Correspondence: liuhongbin@hit.edu.cn (H.L.); tinglima@life.kyutech.ac.jp (T.M.)

Abstract: Large-scale popularization and application make the role of lithium-ion batteries increasingly prominent and the requirements for energy density have increased significantly. The silicon-based material has ultra-high specific capacity, which is expected in the construction of next-generation high specific-energy batteries. In order to improve conductivity and maintain structural stability of the silicon anode in application, and further improve the energy density of the lithium-ion battery, we designed and synthesized carbon-coated porous silicon structures using diatomite and polysaccharides as raw materials. The electrode materials constructed of diatomite exhibit porous structures, which can provide fast transport channels for lithium ions, and effectively release the stress caused by volume expansion during cycling. At the same time, the electrical conductivity of the materials has been significantly improved by compounding with biomass carbon, so the batteries exhibit stable electrochemical performance. We systematically studied the effect of different contents of biomass carbon on the $\text{Li}_2\text{MnSiO}_4/\text{C}$ cathode, and the results showed that the carbon content of 20% exhibited the best electrochemical performance. At a current density of 0.05C, the capacity close to 150 mAh g^{-1} can be obtained after 50 cycles, which is more than three times that of without biomass carbon. The silicon-based anode composited with biomass carbon also showed excellent cycle stability; it could still have a specific capacity of 1063 mAh g^{-1} after 100 cycles at the current density of 0.1 A g^{-1} . This study sheds light on a way of synthesizing high specific-capacity electrode materials of the lithium-ion battery from natural raw materials.

Keywords: diatomite; lithium-ion batteries; $\text{Li}_2\text{MnSiO}_4/\text{C}$ cathode; natural raw materials



Citation: Chen, Y.; Jiang, B.; Zhao, Y.; Liu, H.; Ma, T. Diatomite and Glucose Bioresources Jointly Synthesizing Anode/Cathode Materials for Lithium-Ion Batteries. *Coatings* **2023**, *13*, 146. <https://doi.org/10.3390/coatings13010146>

Academic Editor: Alessandro Latini

Received: 30 November 2022

Revised: 3 January 2023

Accepted: 7 January 2023

Published: 11 January 2023



Copyright: © 2023 by the authors. Licensee MDPI, Basel, Switzerland. This article is an open access article distributed under the terms and conditions of the Creative Commons Attribution (CC BY) license (<https://creativecommons.org/licenses/by/4.0/>).

1. Introduction

With the development of modern industry and human society, fossil energy is depleted day by day, and environmental issues have received increasing attention. Researchers have begun to turn their attention to renewable and clean energy such as solar energy, tidal energy, and wind energy, etc. Secondary batteries, fuel cells, and supercapacitors are the most common high-efficiency energy storage devices [1–3]. Among these, secondary batteries stand out due to their high energy density, strong environmental adaptability, and wide application range [4,5]. In recent years, lithium-ion batteries have been widely used in portable electronic devices, electric vehicles, household power supply, etc. With the popularity of electric vehicles, the demand for lithium-ion batteries has particularly surged. Therefore, lithium-ion batteries with higher energy density, lower cost, and stable operation are the source of high hopes [6]. At the same time, as an important part of the battery, the synthesis of electrode materials with high, specific energy and low cost is an important area of research [7].

In recent years, researchers have begun to use bio-renewable and sustainable source raw materials to synthesize electrode materials for reducing environmental damage caused by waste [8–10]. Before that, biomass materials with multifarious and abundant resources have been widely used in electrical energy storage, electrocatalysis, photocatalysis, multi-phase catalysis, bio-fuel environment, etc. [11,12]. Currently, biomass and biowaste-based carbon materials as anode materials for lithium-ion batteries have received extensive attention due to the advantages of being inexpensive, abundant, and environmentally friendly [13,14]. The basic elements of carbon, sulfur, nitrogen, and phosphorus can increase the wettability and reduce the transfer resistance of the biomass-derived carbon material, which contributes to the increase in battery capacity [15]. Meanwhile, biomass-derived carbon materials possess naturally ordered unique hierarchical structures as well as abundant surface properties and active sites, which facilitate ion transfer and diffusion [16,17]. Thus, research has been conducted on the use of low-cost, environmentally friendly biomass materials to synthesize electrode materials for lithium-ion batteries [18]. The electrode materials that have been reported to use biomass synthesis include rice husks, bamboo leaves, diatomite, etc. [19,20].

Diatomite is a bio-deposited siliceous rock formed from diatom remains over a long period of time in the natural environment; it is mainly composed of amorphous protein minerals of SiO_2 [21,22]. Diatomite is non-toxic, high in purity, and low in acquisition cost. Natural diatoms have different shapes, resulting in the formation of diatomite showing a variety of different microscopic forms, mostly in the shape of a round sieve, a column, or a belt [23–25]. The wall shell of diatomite is composed of multi-level, large, and orderly arranged micropores which are widely used as reaction catalysts, fillers, thermal insulation materials, and filter materials due to the properties of being lightweight, porous, with a large specific surface area, and a strong adsorption capacity [26,27].

Among the electrode materials of lithium-ion batteries, $\text{Li}_2\text{MnSiO}_4$ (LMS) cathode electrode material and Si anode electrode material have been reported with high energy density [28,29]. For cathode materials, $\text{Li}_2\text{MnSiO}_4$ has high theoretical capacitance (333 mA hg^{-1}) and excellent thermal stability due to the Si–O covalent bond [30,31]. Silicon is one of the most valuable anode materials of lithium-ion battery because it has a high theoretical capacity ($\sim 4200 \text{ mA hg}^{-1}$), low working potential, is an abundant resource, and is environmentally friendly [32–34]. Both of these materials can be synthesized using diatomite, so the cost can be effectively reduced. However, the silicon anode electrode has a large volume of more than 400% due to charging and discharging. Therefore, it is necessary to modify the material in a suitable way in order to bring out the advantages of the silicon anode [35–37]. Researchers have explored a variety of strategies to solve the issues, such as designing the structure of silicon materials which contain nano-silicon, layered silicon, porous silicon, etc. Another more effective way is to compound silicon with other materials to maintain the stability of silicon in the cycle, which contains carbon, metal oxide, sulfide, two-dimensional materials, etc. [38–40]. Glucose is a good carbon source that can build a three-dimensional conductive carbon network inside the materials, further improving the electronic conductivity of the materials [41,42].

In this work, we synthesized a diatomite-derived $\text{Li}_2\text{MnSiO}_4/\text{C}$ cathode electrode material and a Si/C anode electrode material with excellent electrochemical performance. New smaller holes could be generated between the diatomaceous earth particles during the preparation of the Si material. In addition, the fabricated anode material maintained a discharge capacity of 1063 mAh g^{-1} after 100 cycles, showing excellent electrical performance and good stability. While the expansion and increase in internal resistance of the anode material can be suppressed, both the capacity retention rate and the coulombic efficiency can be improved. The $\text{Li}_2\text{MnSiO}_4/\text{C}$ cathode also delivered a specific capacity of 249.3 mAh g^{-1} in the first cycle and maintained a specific capacity of about 150 mAh g^{-1} after 50 cycles were compared. The results show that the synthesized $\text{Li}_2\text{MnSiO}_4/\text{C}$ cathode material has good electrochemical performance and stability. For most lithium electrode materials, although a high capacity can be achieved, the extraction process is highly compli-

cated and costly. We used low-cost diatomite as a precursor to synthesize lithium electrode materials and obtained a higher theoretical capacity for the first time. This study provides a strong candidate for the utilization of environmentally friendly biomass towards efficient energy storage through facile and low-cost procedures.

2. Materials and Methods

All chemicals were of analytical grade and used as received without further purification. Diatomite (Wako, 99%), $\text{MnCO}_3 \cdot n\text{H}_2\text{O}$ (Wako, 99%), $\text{LiOH} \cdot \text{H}_2\text{O}$ (Wako, 99%), Mg (Wako, 99%), and NaCl (Wako, 99%).

2.1. Fabrication of Cathode Electrode $\text{Li}_2\text{MnSiO}_4/\text{C}$

Diatomite was treated with 1M HCl solution to obtain high purity SiO_2 . The obtained SiO_2 , $\text{MnCO}_3 \cdot n\text{H}_2\text{O}$, and $\text{LiOH} \cdot \text{H}_2\text{O}$ were individually, finely pulverized in an agate mortar for 30 min. Then, the various processed materials were mixed together and ground for another 15 min. Next, the mixed sample was added to the ethanol solution and stirred thoroughly for dispersion for 6 h. After vacuum drying, calcining in tube furnace for 8 h under argon atmosphere at 700 °C, the $\text{Li}_2\text{MnSiO}_4$ material was obtained. Finally, the glucose was added to $\text{Li}_2\text{MnSiO}_4$ material to obtain different proportions of carbon (weight ratio 0%, 10%, 20%) by calcining in tube furnace for 2 h under argon atmosphere at 600 °C to prepare three cathode materials of LMS/wt.0% C, LMS/wt.10% C, and LMS/wt.20% C.

2.2. Fabrication of Anode Electrode Si/C

First, the treated diatomite, Mg powder, and NaCl were ground in an agate mortar for 30 min. The mixing sample was calcined in the tube furnace for 8 h under argon atmosphere at 700 °C [43]. Then, the argon was replaced with nitrogen and calcined for another 8 h. Next, the obtained sample was added to 1M HCl solution to remove impurities to obtain porous silicon material. After compounding with glucose, carbonizing for 2 h under argon atmosphere at 600 °C, the final Si/C anode material with carbon content of 10% was obtained (DS-3). The additional samples DS-1 (without NaCl and N_2 process) and DS-2 (without N_2 process) were also prepared according to different conditions.

The synthesis procedure is shown in Figure 1.

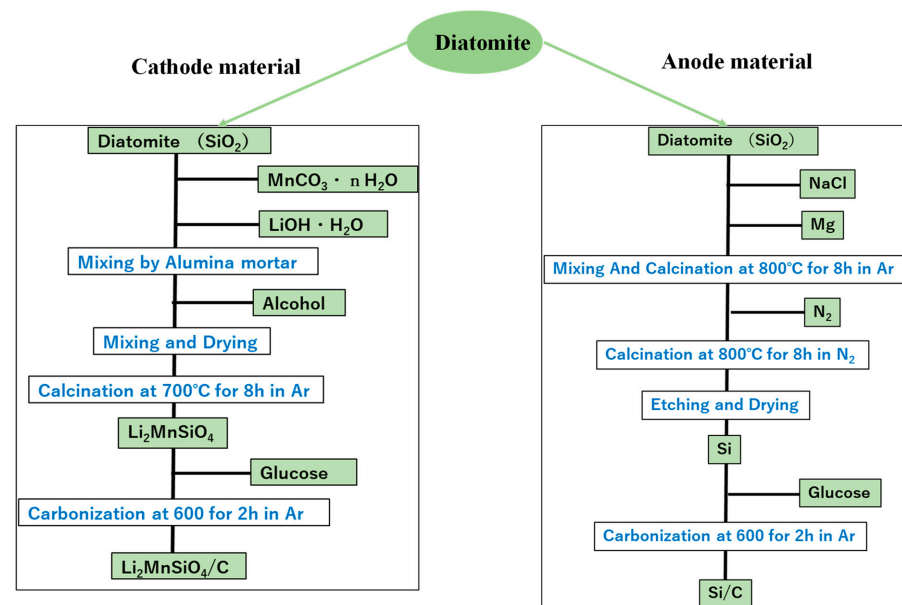


Figure 1. Synthesis process of $\text{Li}_2\text{MnSiO}_4/\text{C}$ and Si/C materials.

2.3. Fabrication of Coin Batteries

The active materials, conductive additive acetylene black, and polyvinylidene difluoride (PVDF) were mixed with NMP at a ratio of 80:10:10 to form homogenous slurries. The slurries were coated on aluminum foil for cathode material and copper foil for anode material. The obtained electrodes were dried at 90 °C for 2 h, and then transferred to vacuum oven at 120 °C for 10 hours. The mass loading of active materials in the working electrodes was 1.0–1.5 mg/cm², with lithium metal as the counter electrode. The 2032 type button batteries were manufactured using the manufactured electrodes. The microporous polypropylene membrane was used as a separator. The electrolyte was 1 M LiPF₆ in a mixed ethylene carbonate/diethyl carbonate solvent (1:1) with 5% fluoroethylene carbonate (FEC) additive.

3. Results and Discussion

3.1. Morphology Characteristics

The scanning electron microscope (SEM) measurement was used to observe and analyze the characteristics of material morphology, as shown in Figure 2. The diatomite we used has a complete shape, and the micropores on the wall are uniform in size and arranged in an orderly manner. It is an exquisite natural porous material (Figure 2a). The diatomite in the shape of a round cake has a rich and well-developed honeycomb porous structure (Figure 2b). Thus, the large specific surface area of diatomite is conducive to the embedding of lithium ions, and the porous circular cake structure can provide more buffer space to enhance the stability. The Si/C anode material obtained by reducing diatomite maintains the characteristics, and the surface is rougher from the increased porous structure (Figure 2c,d). This special structure can maintain the structural stability of the Si-based material during cycling, which was also proved by subsequent electrochemical tests. The surface morphology of Li₂MnSiO₄/C cathode material is different from the original diatomite. The observed void structure is significantly smaller, and the surface has obvious granularity (Figure 2e,f). This is mainly because the synthesis process of Li₂MnSiO₄/C cathode material is an “addition” reaction, which is different from the diatomite-based “reduction” reaction of the Si/C anode material in the reaction process.

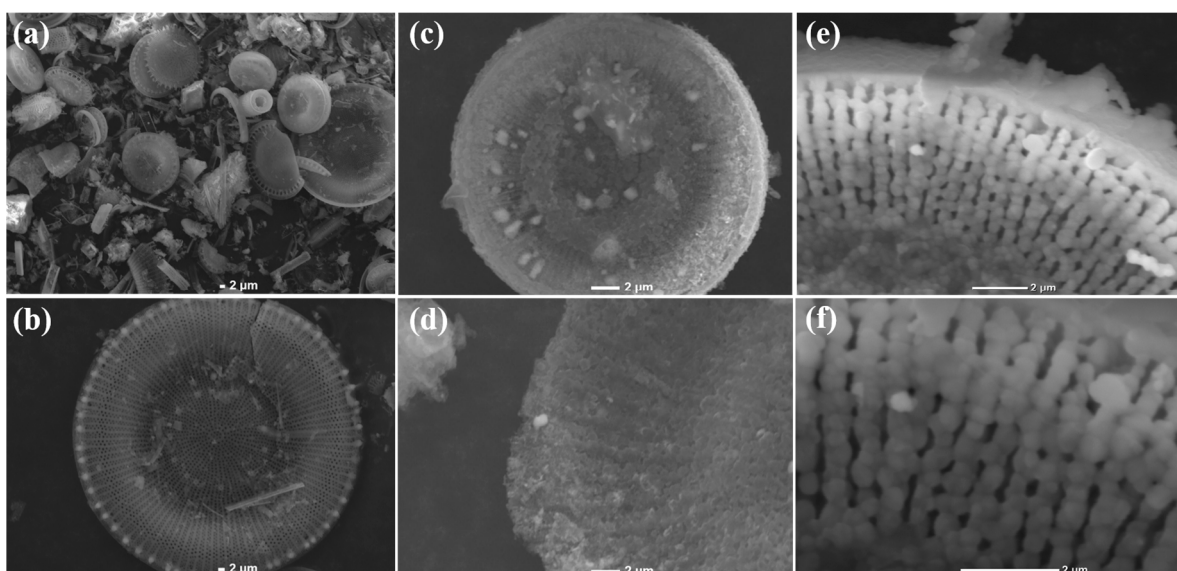


Figure 2. The SEM images of (a,b) diatomite, (c,d) Si/C anode material, and (e,f) Li₂MnSiO₄/C cathode material.

Transmission electron microscopy (TEM) and energy-dispersive X-ray spectroscopy (EDX) were used to further analyze the structure of the samples on a smaller scale, which is shown in Figures 3 and 4. It shows that the Li₂MnSiO₄/C cathode material is composed of

100 nm~200 nm particles (Figure 3a,b). EDX element mapping displays that the elements of O, Si, and Mn are evenly distributed on the surface of the $\text{Li}_2\text{MnSiO}_4/\text{C}$ composite (Figure 3c–e). And the Si/C anode material is distributed with a porous structure and with Si elements uniformly distributed (Figure 4).

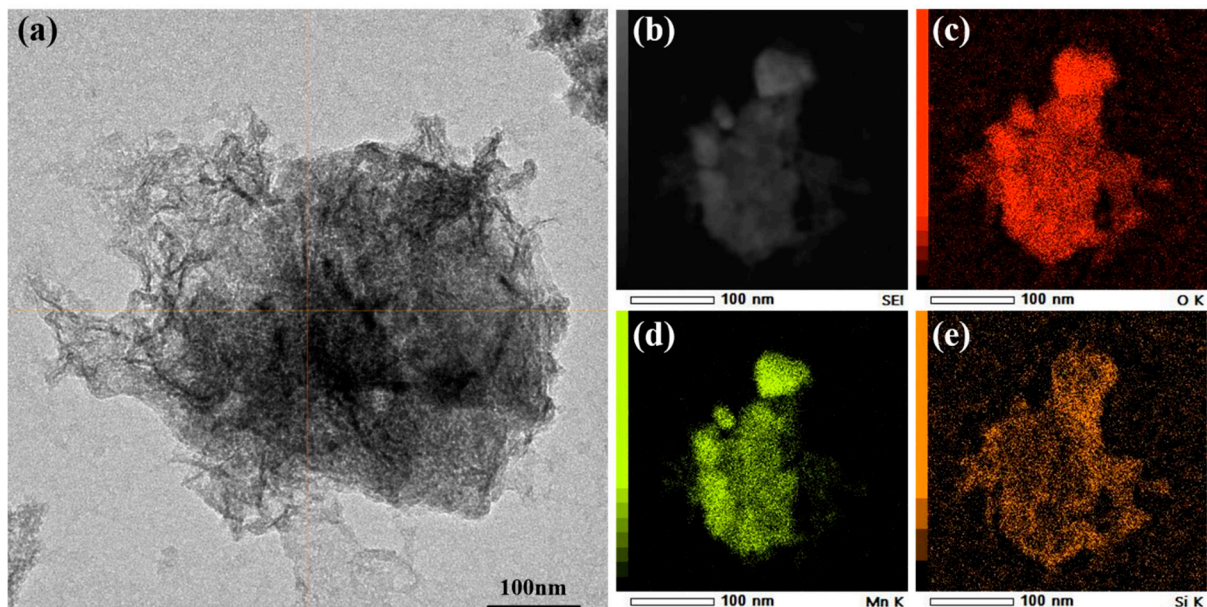


Figure 3. The (a,b) TEM images of $\text{Li}_2\text{MnSiO}_4/\text{C}$ cathode material; the EDX mapping images: (c) O, (d) Mn, and (e) Si elements distribution.

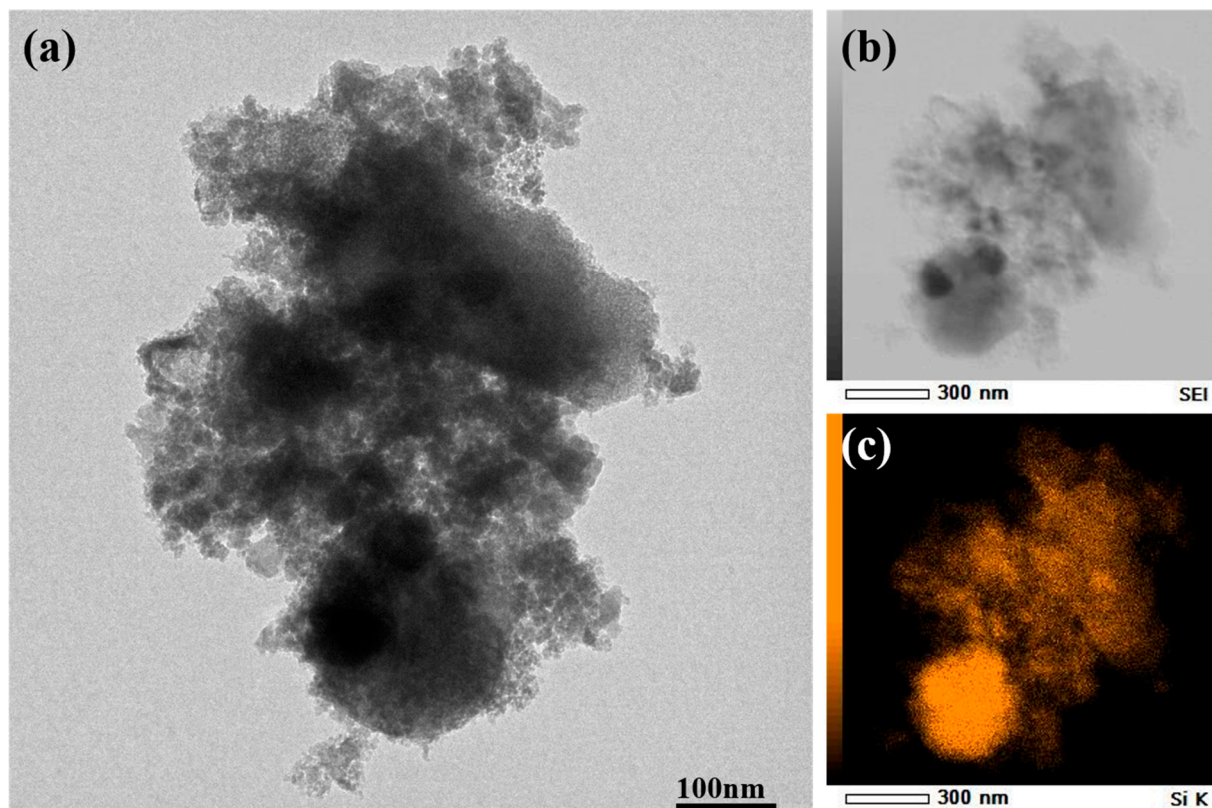


Figure 4. The (a,b) TEM images and (c) EDX mapping image of Si/C anode material.

3.2. Structural Characteristics

The X-ray diffraction (XRD) patterns were used to determine the main composition of the $\text{Li}_2\text{MnSiO}_4/\text{C}$ cathode and Si/C anode. It was found that the XRD pattern of $\text{Li}_2\text{MnSiO}_4/\text{C}$ contained an impure phase that belonged to MnO as shown in Figure 5a. However, other characteristic peaks are consistent with the pure $\text{Li}_2\text{MnSiO}_4$ phase. Figure 5b shows the XRD diffraction patterns of different Si/C anode materials prepared by changing the synthesis conditions. The characteristic peaks at 76.7° , 69° , 56.2° , 47.4° , and 28.5° are attributed to the (331), (400), (311), (220), and (111) of pure silicon lattice planes, respectively [34]. Therefore, it was confirmed that there are no other impurities in the synthesized samples.

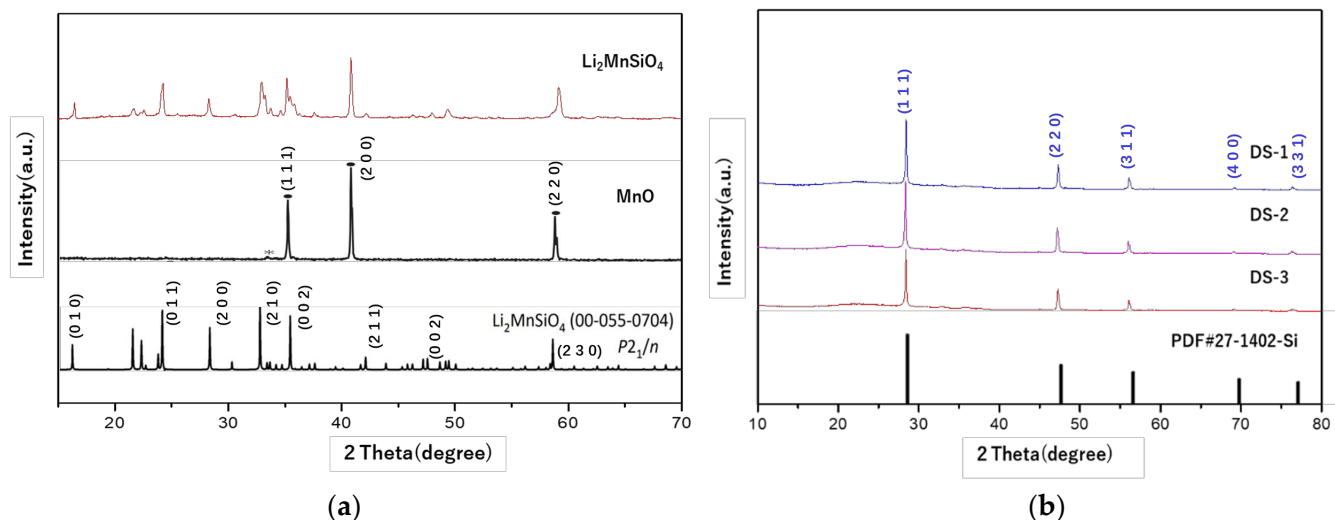


Figure 5. (a) The XRD patterns of $\text{Li}_2\text{MnSiO}_4/\text{C}$ cathode and (b) Si/C anode.

The specific surface area and pore volume of the samples were measured by the N_2 adsorption method based on Brunauer–Emmett–Teller (BET), which is shown in Figure 6 and Table 1. The diatomite has a specific surface area of $32.6 \text{ m}^2 \text{ g}^{-1}$, while the specific surface area of the $\text{Li}_2\text{MnSiO}_4/\text{C}$ cathode material is reduced by about five times to $6.4 \text{ m}^2 \text{ g}^{-1}$ (Figure 6a). Due to the generated internal “addition” reaction with the $\text{MnCO}_3 \cdot n\text{H}_2\text{O}$ and $\text{LiOH} \cdot \text{H}_2\text{O}$, the mass of diatomite increases, which will significantly reduce the size of the structural pores, which is also confirmed by the SEM. Different from the $\text{Li}_2\text{MnSiO}_4/\text{C}$ cathode material, the specific surface areas of the synthesized anode materials DS-1, DS-2, and DS-3 increase to 137.6 , 160.6 , and $253.0 \text{ m}^2 \text{ g}^{-1}$, respectively. As a result of the “reduction” reaction, the oxygen atoms in the diatomite are released, and more space is reserved in the structure.

Table 1. BET measurement result of materials.

	Material	Specific Surface Area/ $\text{m}^2 \text{ g}^{-1}$	Pore Volume/ $\text{m}^3 \text{ g}^{-1}$
Precursor	Diatomite	32.6	0.05
Cathode	$\text{Li}_2\text{MnSiO}_4/\text{C}$	6.4	0.01
Anode	DS-1	137.6	0.18
	DS-2	160.6	0.56
	DS-3	253.0	1.07

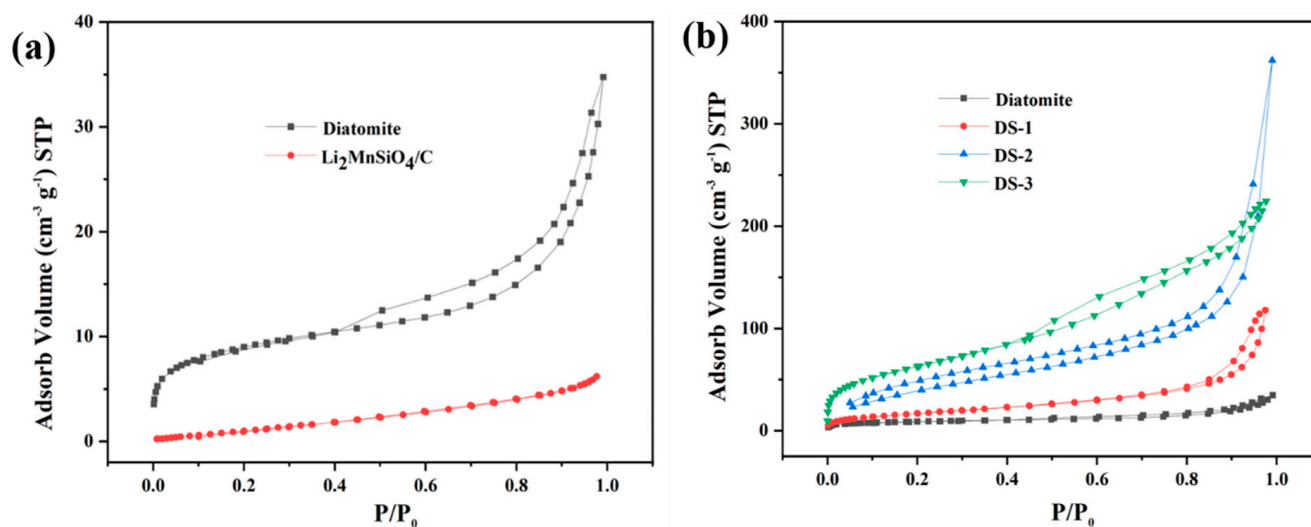


Figure 6. The nitrogen adsorption–desorption isotherms of (a) diatomite and Li₂MnSiO₄/C; and (b) DS-1, DS-2, and DS-3.

3.3. Electrochemical Performance

The cyclic voltammetry (CV) curves of the Li₂MnSiO₄/C cathode and the DS-3 anode are shown in Figure 7. For Li₂MnSiO₄/C cathode, the peaks around 3.6 V and 4.3 V at the cathodic scan are due to the conversion reaction of Mn²⁺ to Mn³⁺ and Mn⁴⁺. The peaks at 2.0 V, 2.8 V, and 4.4 V at the cathodic scan are due to the reversible reduction of Mn⁴⁺ to Mn²⁺ (Figure 7a). Figure 7b shows the redox curve of a typical Si-based anode. The cathodic peak at 0.1 V corresponds to the formation of an amorphous Si–Li alloy, while two anodic peaks at 0.25 and 0.5 V are due to the conversion reaction of Li_xSi to amorphous Si. Figure 7c shows the charge–discharge curves of Li₂MnSiO₄/C with different carbon content during the first cycle at a current density of 0.05C. The discharge capacity of LMS/wt.0% C is 187.4 mAhg⁻¹, which is 59% of the charge capacity of 318.2 mAhg⁻¹, while the LMS/wt.10% C and LMS/wt.20% cathode exhibit over 80% initial coulomb efficiency. Figure 7d shows the cycle curves of Li₂MnSiO₄/C cathode materials at a current density of 0.05C. Compared to LMS/wt.0% C and LMS/wt.10% C, LMS/wt.20% C has the best electrochemical performance. For LMS/wt.20% C, the specific capacity is about 150 mAh g⁻¹ after 50 cycles, which proved it has stable cycling performance. The results of LMS/wt.10% C and LMS/wt.20% proved that combining with carbon is an effective way to improve the conductivity of the Li₂MnSiO₄ cathode. Figure 7e shows the cycle curves of the Si/C anode. After 100 cycles, the discharge specific capacity of the DS-3 anode is 1063 mA h g⁻¹, which is much superior to DS-1 and DS-2. This is due to the fact that the original shape and porous structure of diatomite are maintained during the synthesis process. In addition, the participation of N₂ is conducive to the generation of porous structure which provides more buffer space for the expansion of the Si-based anode during cycling. At the same time, the rate capability test is also used to confirm the performance of Si/C anode materials at different current densities (Figure 7f). As expected, the DS-3 anode material exhibits the best rate performance, and when the current density returned to 100 mA g⁻¹, its specific capacity returned to above 1000 mAh g⁻¹.

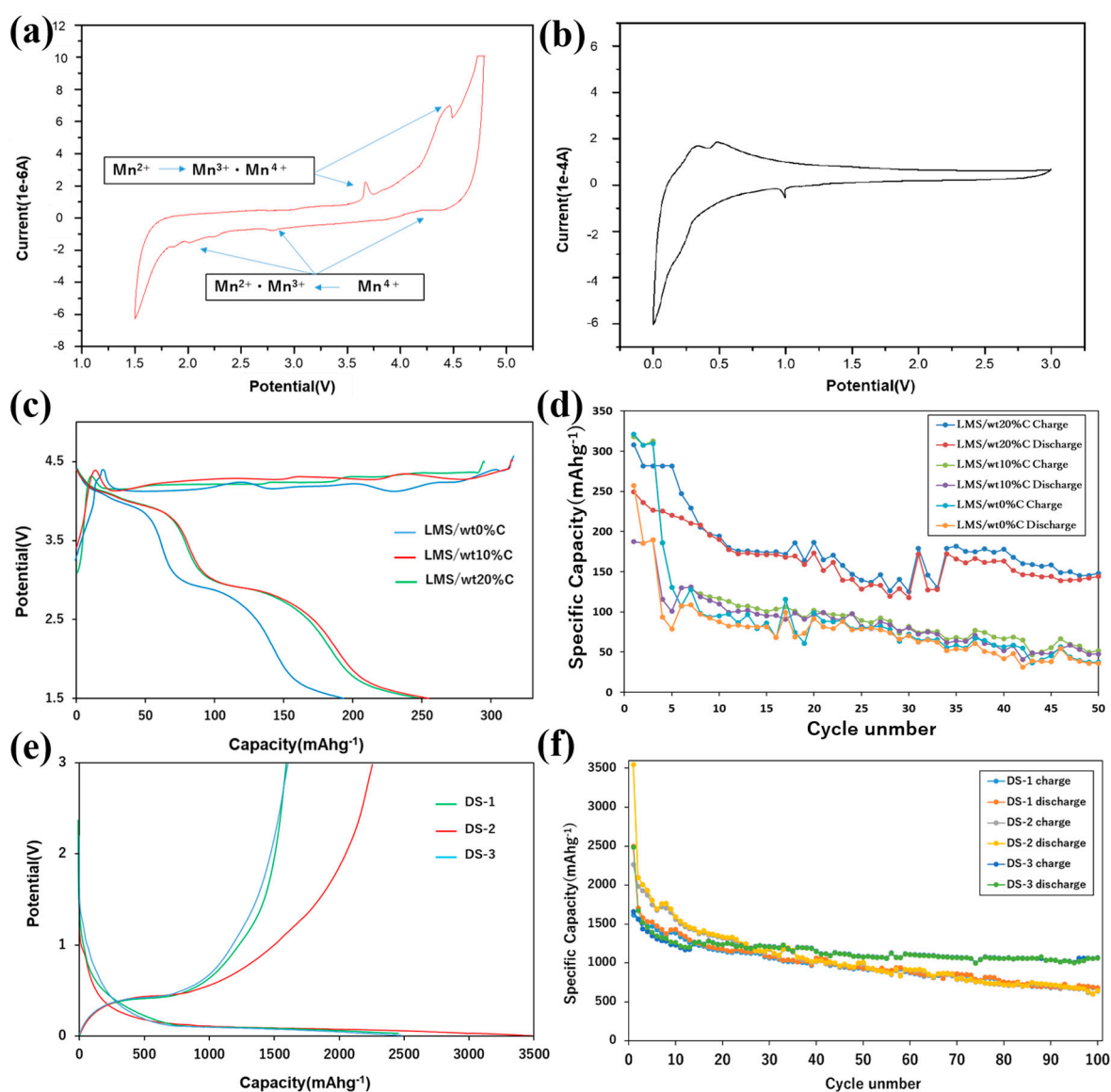


Figure 7. The CV curves of (a) $\text{Li}_2\text{MnSiO}_4/\text{C}$ cathode under the potential range from 1.5 to 4.8 V and (b) DS-3 anode under the potential range from 0.005 to 3.0 V at 0.1 mV/s. (c) Charge/discharge curve diagram and (d) cycling performance of $\text{Li}_2\text{MnSiO}_4$ cathode under the potential range from 1.5 to 4.5 V at a current density of 0.05C. (e) Charge/discharge curve diagram and (f) cycling performance of Si/C anode materials under the potential range from 0.005 to 3.0 V at a current density of 0.1 A g^{-1} .

4. Conclusions

In this work, we designed and synthesized a porous $\text{Li}_2\text{MnSiO}_4/\text{C}$ cathode and Si/C anode materials using natural diatomite and glucose. By compounding, the electrical conductivity of the materials is significantly improved, and the porous structures of the materials can effectively maintain stability. Through gradient comparison, the $\text{Li}_2\text{MnSiO}_4/\text{C}$ cathode material prepared with 20% glucose has better electrochemical performance and capacity retention after 50 cycles. With a simple mixed calcination treatment, we obtained a stable Si/C anode material with high specific capacity. After different conditions and comparisons, we screened out the best reaction conditions. By mixing NaCl and adding a step of nitrogen calcination, the treated materials react more fully, the impurities can be effectively removed, and a purer product sample DS-3 can be obtained which has a smaller particle size distribution. It has a larger specific surface area of $253 \text{ m}^2 \text{ g}^{-1}$ while still maintaining a porous structure, which has a positive effect on the fast transport of lithium ions. Thus, the cycling performance of the material can be improved. After 100 cy-

cles, the material can maintain the capacity of above 1000 mAh g⁻¹ at the current density of 100 mA g⁻¹. This provides a very good reference for the use of natural materials to construct high specific-energy lithium-ion batteries.

Author Contributions: Methodology, B.J.; Software, Y.Z.; Investigation, Y.C. and B.J.; Data curation, Y.Z.; Writing—original draft, Y.C., H.L. and T.M.; Writing—review & editing, H.L. and T.M. All authors have read and agreed to the published version of the manuscript.

Funding: This work was conducted at Kitakyushu Foundation for the Advancement of Industry, Science and Technology, Semiconductor Center, and supported by “Nanotechnology Platform Program” of the Ministry of Education, Culture, Sports, Science and Technology (MEXT), Japan, Grant Number JPMXP09F-19-FA-0029 and KAGENHI Grant-in-Aid for Scientific Research(B), No.19H02818, and the National Natural Science Foundation of China (Grant No. 51772039 and 51972293).

Institutional Review Board Statement: Not applicable.

Informed Consent Statement: Not applicable.

Data Availability Statement: Not applicable.

Conflicts of Interest: The authors declare no conflict of interest.

References

1. Duffner, F.; Kronemeyer, N.; Tübke, J.; Leker, J.; Winter, M.; Schmich, R. Post-lithium-ion battery cell production and its compatibility with lithium-ion cell production infrastructure. *Nat. Energy* **2021**, *6*, 123–134. [[CrossRef](#)]
2. Xiong, R.; Pan, Y.; Shen, W.; Li, H.; Sun, F. Lithium-ion battery aging mechanisms and diagnosis method for automotive applications: Recent advances and perspectives. *Renew. Sustain. Energy Rev.* **2020**, *131*, 110048. [[CrossRef](#)]
3. Sasrimuang, S.; Chuchuen, O.; Artnaseaw, A. Synthesis, characterization, and electrochemical properties of carbon nanotubes used as cathode materials for Al–air batteries from a renewable source of water hyacinth. *Green Process. Synth.* **2020**, *9*, 340–348. [[CrossRef](#)]
4. Lyu, P.; Liu, X.; Qu, J.; Zhao, J.; Huo, Y.; Qu, Z.; Rao, Z. Recent advances of thermal safety of lithium ion battery for energy storage. *Energy Storage Mater.* **2020**, *31*, 195–220. [[CrossRef](#)]
5. Pushnitsa, K.; Kosenko, A.; Chernyavsky, V.; Pavlovskii, A.A.; Novikov, P.; Popovich, A.A. Copper-Coated Graphite Felt as Current Collector for Li-Ion Batteries. *Coatings* **2022**, *12*, 1321. [[CrossRef](#)]
6. Sommerville, R.; Zhu, P.; Rajaeifar, M.A.; Heidrich, O.; Goodship, V.; Kendrick, E. A qualitative assessment of lithium ion battery recycling processes. *Resour. Conserv. Recycl.* **2021**, *165*, 105219. [[CrossRef](#)]
7. Liu, K.; Wei, Z.; Yang, Z.; Li, K. Mass load prediction for lithium-ion battery electrode clean production: A machine learning approach. *J. Clean. Prod.* **2021**, *289*, 125159. [[CrossRef](#)]
8. Chen, Y.; Liu, H.; Jiang, B.; Zhao, Y.; Meng, X.; Ma, T. Hierarchical porous architectures derived from low-cost biomass equisetum arvense as a promising anode material for lithium-ion batteries. *J. Mol. Struct.* **2020**, *1221*, 128794. [[CrossRef](#)]
9. Zhang, Y.; Zhang, R.; Chen, S.; Gao, H.; Li, M.; Song, X.; Xin, H.L.; Chen, Z. Diatomite-Derived Hierarchical Porous Crystalline-Amorphous Network for High-Performance and Sustainable Si Anodes. *Adv. Funct. Mater.* **2020**, *30*, 2005956. [[CrossRef](#)]
10. Wu, W.; Wang, M.; Wang, J.; Wang, C.; Deng, Y. Green Design of Si/SiO₂/C Composites as High-Performance Anodes for Lithium-Ion Batteries. *ACS Appl. Energy Mater.* **2020**, *3*, 3884–3892. [[CrossRef](#)]
11. Shibutani, N.; Sugiura, K.; Tanaka, A.; Nagato, K. Examination on Water Management Method in the Same Electrode in PEFC. *ECS Trans.* **2021**, *104*, 243. [[CrossRef](#)]
12. Ribeiro, M.J.; Tulyaganov, D.U.; Ferreira, J.M.F.; Labrincha, J.A. Production of Al-rich sludge-containing ceramic bodies by different shaping techniques. *J. Mater. Process. Technol.* **2004**, *148*, 139–146. [[CrossRef](#)]
13. Nie, W.; Cheng, H.; Liu, X.; Sun, Q.; Tian, F.; Yao, W.; Liang, S.; Lu, X.; Zhou, J. Surface organic nitrogen-doping disordered biomass carbon materials with superior cycle stability in the sodium-ion batteries. *J. Power Sources* **2022**, *522*, 230994. [[CrossRef](#)]
14. Dominko, R.; Bele, M.; Gaberšček, M.; Meden, A.; Remškar, M.; Jamnik, J. Structure and electrochemical performance of Li₂MnSiO₄ and Li₂FeSiO₄ as potential Li-battery cathode materials. *Electrochem. Commun.* **2006**, *8*, 217–222. [[CrossRef](#)]
15. Wang, P.; Chen, L.; Shen, Y. Recycling spent ternary lithium-ion batteries for modification of dolomite used in catalytic biomass pyrolysis—A preliminary study by thermogravimetric and pyrolysis-gas chromatography/mass spectrometry analysis. *Bioresour. Technol.* **2021**, *337*, 125476. [[CrossRef](#)]
16. Yu, J.; Tang, T.; Cheng, F.; Huang, D.; Martin, J.L.; Brewer, C.E.; Grimm, R.L.; Zhou, M.; Luo, H. Exploring spent biomass-derived adsorbents as anodes for lithium ion batteries. *Mater. Today Energy* **2021**, *19*, 100580. [[CrossRef](#)]
17. Ma, Q.; Dai, Y.; Wang, H.; Ma, G.; Guo, H.; Zeng, X.; Tu, N.; Wu, X.; Xiao, M. Directly conversion the biomass-waste to Si/C composite anode materials for advanced lithium ion batteries. *Chin. Chem. Lett.* **2021**, *32*, 5–8. [[CrossRef](#)]
18. Vernardou, D. Recent Report on the Hydrothermal Growth of LiFePO₄ as a Cathode Material. *Coatings* **2022**, *12*, 1543. [[CrossRef](#)]

19. Guo, X.; Zheng, S.; Luo, Y.; Pang, H. Synthesis of confining cobalt nanoparticles within SiO_x/nitrogen-doped carbon framework derived from sustainable bamboo leaves as oxygen electrocatalysts for rechargeable Zn-air batteries. *Chem. Eng. J.* **2020**, *401*, 126005. [[CrossRef](#)]
20. Chen, Y.; Guo, X.; Liu, A.; Zhu, H.; Ma, T. Recent progress in biomass-derived carbon materials used for secondary batteries. *Sustain. Energy Fuels* **2021**, *5*, 3017–3038. [[CrossRef](#)]
21. Bakr, H. Diatomite: Its characterization, modifications and applications. *Asian J. Mater. Sci.* **2010**, *2*, 121–136.
22. Zhou, F.; Li, Z.; Lu, Y.-Y.; Shen, B.; Guan, Y.; Wang, X.-X.; Yin, Y.-C.; Zhu, B.-S.; Lu, L.-L.; Ni, Y.; et al. Diatomite derived hierarchical hybrid anode for high performance all-solid-state lithium metal batteries. *Nat. Commun.* **2019**, *10*, 2482. [[CrossRef](#)]
23. Ivanov, S.É.; Belyakov, A. Diatomite and its applications. *Glass Ceram.* **2008**, *65*, 18–21. [[CrossRef](#)]
24. Chen, X.; Tian, Y. Review of Graphene in Cathode Materials for Lithium-Ion Batteries. *Energy Fuels* **2021**, *35*, 3572–3580. [[CrossRef](#)]
25. Kang, M.S.; Heo, I.; Kim, S.; Yang, J.; Kim, J.; Min, S.-J.; Chae, J.; Yoo, W.C. High-areal-capacity of micron-sized silicon anodes in lithium-ion batteries by using wrinkled-multilayered-graphenes. *Energy Storage Mater.* **2022**, *50*, 234–242. [[CrossRef](#)]
26. de Namor, A.F.D.; El Gamouz, A.; Frangie, S.; Martinez, V.; Valiente, L.; Webb, O.A. Turning the volume down on heavy metals using tuned diatomite. A review of diatomite and modified diatomite for the extraction of heavy metals from water. *J. Hazard. Mater.* **2012**, *241*, 14–31. [[CrossRef](#)]
27. Caliskan, N.; Kul, A.R.; Alkan, S.; Sogut, E.G.; Alacabey, I. Adsorption of Zinc (II) on diatomite and manganese-oxide-modified diatomite: A kinetic and equilibrium study. *J. Hazard. Mater.* **2011**, *193*, 27–36. [[CrossRef](#)] [[PubMed](#)]
28. Cheng, Q.; He, W.; Zhang, X.; Li, M.; Wang, L. Modification of Li₂MnSiO₄ cathode materials for lithium-ion batteries: A review. *J. Mater. Chem. A* **2017**, *5*, 10772–10797. [[CrossRef](#)]
29. Shree Kesavan, K.; Michael, M.S.; Prabakaran, S.R.S. Facile Electrochemical Activity of Monoclinic Li₂MnSiO₄ as Potential Cathode for Li-Ion Batteries. *ACS Appl. Mater. Interfaces* **2019**, *11*, 28868–28877. [[CrossRef](#)]
30. Singh, M.; Kumar, N.; Sharma, Y. Role of impurity phases present in orthorhombic-Li₂MnSiO₄ towards the Li-reactivity and storage as LIB cathode. *Appl. Surf. Sci.* **2022**, *574*, 151689. [[CrossRef](#)]
31. Wu, X.; Zhao, S.-X.; Yu, L.-Q.; Yang, J.-L.; Nan, C.-W. Effect of sulfur doping on structural reversibility and cycling stability of a Li₂MnSiO₄ cathode material. *Dalton Trans.* **2018**, *47*, 12337–12344. [[CrossRef](#)]
32. Zhu, P.; Gastol, D.; Marshall, J.; Sommerville, R.; Goodship, V.; Kendrick, E. A review of current collectors for lithium-ion batteries. *J. Power Sources* **2021**, *485*, 229321. [[CrossRef](#)]
33. Li, J.; Xu, J.; Xie, Z.; Gao, X.; Zhou, J.; Xiong, Y.; Chen, C.; Zhang, J.; Liu, Z. Diatomite-Templated Synthesis of Freestanding 3D Graphdiyne for Energy Storage and Catalysis Application. *Adv. Mater.* **2018**, *30*, 1800548. [[CrossRef](#)]
34. Liu, H.; Meng, X.; Chen, Y.; Zhao, Y.; Guo, X.; Ma, T. Synthesis and Surface Engineering of Composite Anodes by Coating Thin-Layer Silicon on Carbon Cloth for Lithium Storage with High Stability and Performance. *ACS Appl. Energy Mater.* **2021**, *4*, 6982–6990. [[CrossRef](#)]
35. Liu, Z.; Lu, D.; Wang, W.; Yue, L.; Zhu, J.; Zhao, L.; Zheng, H.; Wang, J.; Li, Y. Integrating Dually Encapsulated Si Architecture and Dense Structural Engineering for Ultrahigh Volumetric and Areal Capacity of Lithium Storage. *ACS Nano* **2022**, *16*, 4642–4653. [[CrossRef](#)] [[PubMed](#)]
36. Tong, L.; Long, K.; Chen, L.; Wu, Z.; Chen, Y. High-Capacity and Long-Lived Silicon Anodes Enabled by Three-Dimensional Porous Conductive Network Design and Surface Reconstruction. *ACS Appl. Energy Mater.* **2022**, *5*, 13877–13886. [[CrossRef](#)]
37. Zheng, P.; Sun, J.; Liu, H.; Wang, R.; Liu, C.; Zhao, Y.; Li, J.; Zheng, Y.; Rui, X. Microstructure Engineered Silicon Alloy Anodes for Lithium-Ion Batteries: Advances and Challenges. *Batter. Supercaps* **2022**. [[CrossRef](#)]
38. Kim, J.; Park, Y.K.; Kim, H.; Jung, I.H. Ambidextrous Polymeric Binder for Silicon Anodes in Lithium-Ion Batteries. *Chem. Mater.* **2022**, *34*, 5791–5798. [[CrossRef](#)]
39. Li, L.; Li, T.; Sha, Y.; Ren, B.; Zhang, L.; Zhang, S. A Web-like Three-dimensional Binder for Silicon Anode in Lithium-ion Batteries. *Energy Environ. Mater.* **2022**, e12482. [[CrossRef](#)]
40. Liu, P.; Li, B.; Zhang, J.; Jiang, H.; Su, Z.; Lai, C. Self-swelling derived frameworks with rigidity and flexibility enabling high-reversible silicon anodes. *Chin. Chem. Lett.* **2022**, 107946. [[CrossRef](#)]
41. Bai, J.; Zhao, B.; Zhou, J.; Si, J.; Fang, Z.; Li, K.; Ma, H.; Dai, J.; Zhu, X.; Sun, Y. Glucose-induced synthesis of 1T-MoS₂/C hybrid for high-rate lithium-ion batteries. *Small* **2019**, *15*, 1805420. [[CrossRef](#)] [[PubMed](#)]
42. Liu, H.; Luo, S.; Yan, S.; Wang, Q.; Hu, D.; Wang, Y.; Feng, J.; Yi, T. High-performance α-Fe₂O₃/C composite anodes for lithium-ion batteries synthesized by hydrothermal carbonization glucose method used pickled iron oxide red as raw material. *Compos. Part B Eng.* **2019**, *164*, 576–582. [[CrossRef](#)]
43. Yoon, T.; Bok, T.; Kim, C.; Na, Y.; Park, S.; Kim, K.S. Mesoporous Silicon Hollow Nanocubes Derived from Metal–Organic Framework Template for Advanced Lithium-Ion Battery Anode. *ACS Nano* **2017**, *11*, 4808–4815. [[CrossRef](#)] [[PubMed](#)]

Disclaimer/Publisher’s Note: The statements, opinions and data contained in all publications are solely those of the individual author(s) and contributor(s) and not of MDPI and/or the editor(s). MDPI and/or the editor(s) disclaim responsibility for any injury to people or property resulting from any ideas, methods, instructions or products referred to in the content.